Plateau 'pop-up' in the great 1897 Assam earthquake

Roger Bilham*† & Philip England†

** CIRES & Geological Sciences, University of Colorado, Boulder, Colorado 80309-0399, USA*
† Earth Sciences, Oxford University, Parks Road, Oxford OX1 3PR, UK

The great Assam earthquake of 12 June 1897 reduced to rubble all masonry buildings within a region of northeastern India roughly the size of England, and was felt over an area exceeding that of the great 1755 Lisbon earthquake[1]. Hitherto it was believed that rupture occurred on a north-dipping Himalayan thrust fault propagating south of Bhutan[2–5]. But here we show that the northern edge of the Shillong plateau rose violently by at least 11 m during the Assam earthquake, and that this was due to the rupture of a buried reverse fault approximately 110 km in length and dipping steeply away from the Himalaya. The stress drop implied by the rupture geometry and the prodigious fault slip of 18 ± 7 m explains epicentral accelerations observed to exceed 1*g* vertically and surface velocities exceeding 3 m s^{-1} (ref. 1). This quantitative observation of active deformation of a 'pop-up' structure confirms that faults bounding such structures can penetrate the whole crust. Plateau uplift in the past 2–5 million years has caused the Indian plate to contract locally by 4 ± 2 mm yr^{-1}, reducing seismic risk in Bhutan but increasing the risk in northern Bangladesh.

Central to our analysis are the long-neglected survey reports of Bond[6] who located and remeasured the original points of the 1862 trigonometrical survey across the Shillong plateau. Despite the discovery, under appalling conditions, of 8 m of uplift and 4 m of displacement of parts of this plateau, his results were dismissed[7], because they failed to meet the triangle closure standards of the Survey of India. Bond, and later Oldham[1], who attempted to interpret the data, suspected that closure errors were caused by continuing movements following the mainshock, an idea that was many years ahead of its time. Oldham, noting the existence of a northward increasing strain gradient in Bond's data, recommended remeasurement of a survey along the northern edge of the plateau, but this was not to occur until 1936[8] (Fig. 1). These northern measurements had a mean error typical of Survey of India accuracies (3.3 μrad), but did not overlap the earlier re-survey and, as in Bond's survey, included neither scale nor azimuth constraints.

The results of the surveys are available as the locations of points[7,9] with their apparent post-seismic displacements, calculated holding fixed two points within each network[1,6,8,10]. We seek the values of these parameters that best fit the observed angle changes. The absence of scale and orientation information permits only the analysis of angular changes[11,10], which we derive from these published data. We treat the angular changes as though they reflect deformation of an elastic half-space, distorted by slip on a single rectangular plane representing the 1897 earthquake. In doing this, we neglect deformation caused by other earthquakes between 1860–69 and 1897 and by post-seismic deformation before the re-surveys.

The surface distortion caused by slip on a buried dislocation can be calculated from nine parameters that describe its geometry and slip[12]. The problem is sufficiently nonlinear that many local minima exist; we therefore sought a global minimum by systematically searching parameter space. Results of this search are contoured in Fig. 2b. The best-fitting solution, in the sense of minimizing the misfits to the angular changes normalized by their uncertainties, corresponds to a slip of 16 m on a fault plane striking ESE for 110 km and dipping SSW at 57° beneath the northern edge of the plateau (Fig. 2); slip on the plane extends from 9 to 45 km beneath the surface, with a rake of 76°.

Several features of the solution are unexpected. First, all previous studies favoured slip on a plane dipping northwards from the south of the plateau. Furthermore, the extension of the rupture plane to

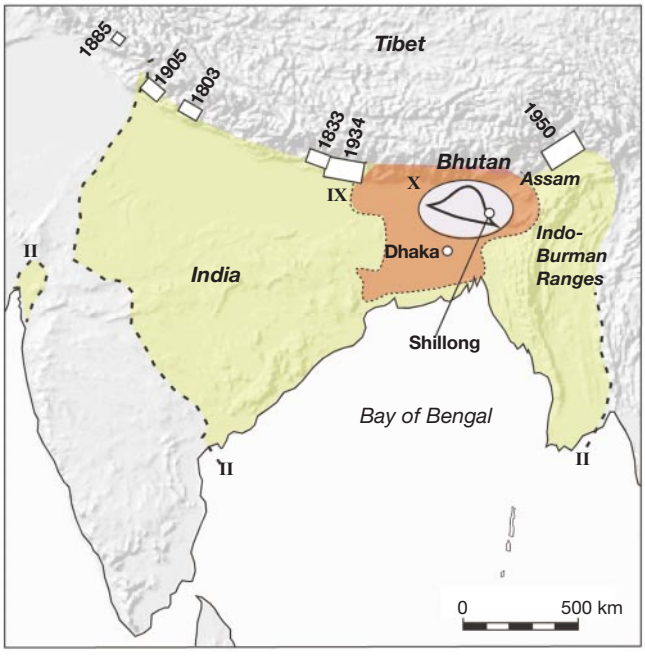

Figure 1 Area shaken by the great 1897 Assam earthquake, and location of major Himalayan ruptures in the past 200 years[30]. Masonry structures were damaged within Oldham's[1] intensity IX contour (orange), and destroyed within the intensity X ellipse (violet). The earthquake was felt by persons within the intensity II region (green). The orientation of the curious 'Mexican-hat' shape of the epicentral region mapped by Oldham corresponds to the strike of the causal subsurface rupture derived from geodetic data (Fig. 2).

the surface corresponds to no mapped fault[13]. In the absence of a named fault we refer to rupture occurring on the 'Oldham fault'. The easternmost edge of the Oldham fault, and the latitude of its western edge, are well constrained by the triangulation data (Fig. 2b). The longitude of the westward termination is consistent with 10 m of up-to-the east vertical slip on the Chedrang fault (Fig. 2). Boundary element[14] calculations treating the Chedrang fault as a frictionless surface driven by coseismic stress changes caused by slip on the Oldham fault emulate the observed distribution of slip only when the ends of the two faults approach within a few kilometres. Finally, the projection of the preferred rupture plane to the surface follows slope breaks on an ESE topographic escarpment along the northern edge of the plateau (Fig. 2c); this projection also follows the strike and location of Oldham's 'Mexican-hat' outline of the rupture zone[1] corresponding to the zone of highest shaking intensity and aftershock productivity[1] (Fig. 1).

Our best-fitting value of 16 m for the slip is one of the greatest for any measured earthquake. A lower bound on the magnitude of this slip comes from the magnitude of the shear strains near the top of the rupture plane (Fig. 2) and, independently, from Oldham's observations on the Chedrang fault, which imply a minimum of 11 m of displacement on the main fault plane. There is a trade-off between the depth of the top of the rupture and the magnitude of

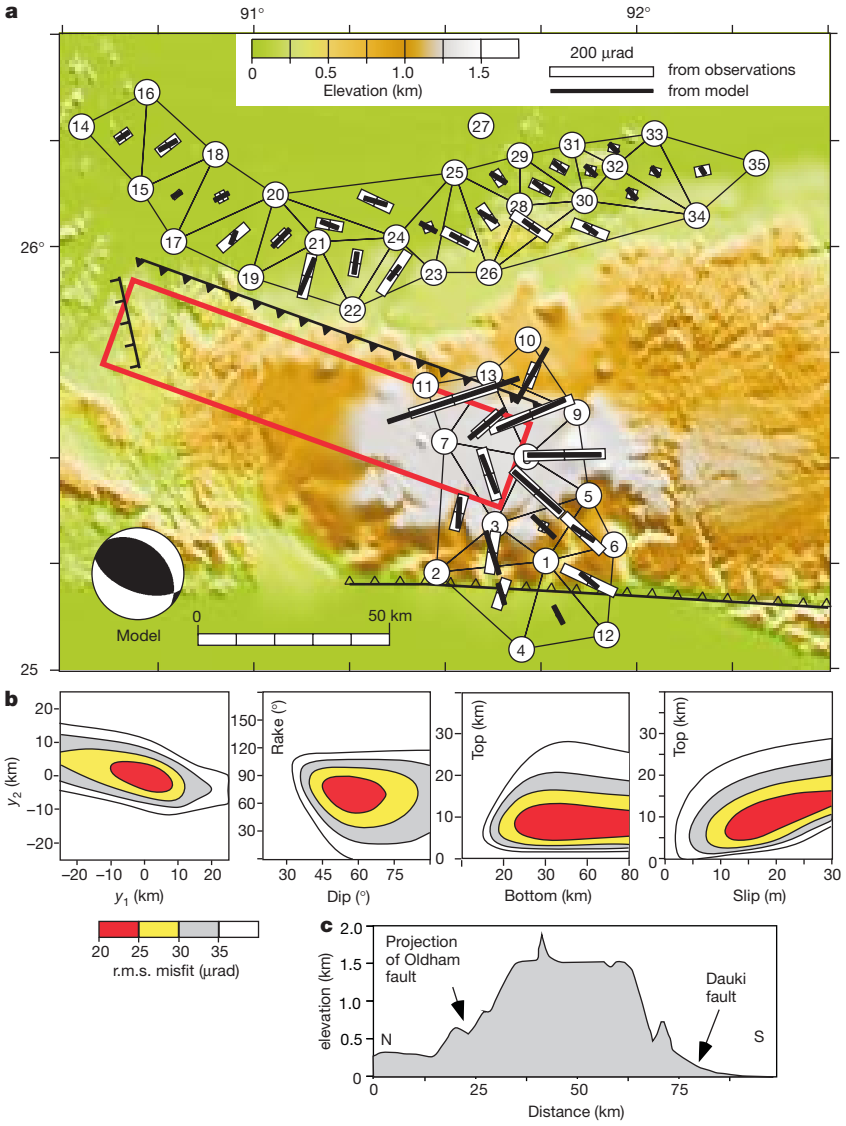

Figure 2 Epicentral region of the Great 1897 Assam earthquake showing geodetic data and inferred rupture plane. **a**, Trigonometrical stations remeasured on[6] and north[8] of the Shillong plateau following the 1897 earthquake. Shear strains for each triangle are displayed as bars whose orientations are parallel to the smallest (most compressional) principal strain and whose lengths are proportional to the shear strain, $\Gamma = (\gamma_1^2 + \gamma_2^2)^{1/2}$ where $\gamma_1 = \delta u/\delta x - \delta v/\delta y$, $\gamma_2 = \delta u/\delta y + \delta v/\delta x$, and u, v are components of displacement in the easterly (x) and northerly (y) directions[11]. White rectangles are calculated for the triangulation observations, and black bars show the strains calculated for the best-fitting planar dislocation. Red rectangle indicates subsurface location of this southwest dipping dislocation; thick black line with filled triangles shows the surface intersection of the continuation of this plane to the land surface (slip terminated 9 km below the surface). Short black line at western edge of fault plane indicates location of Chedrang fault, where Oldham[1] observed 11 m of co-seismic slip down to the west. Line with open triangles to south of the plateau shows location of the Dauki fault. **b**, Trade-offs between parameters of the model dislocation. Each panel displays the variation in root-mean-square misfit to the observed angular changes, with all parameters except those illustrated held fixed to their best-fitting values; y_1 and y_2 refer to latitudinal coordinate of, respectively, the western and eastern ends of the fault. **c**, Topographic section through the central Shillong plateau showing projected surface location of the Oldham fault. A peneplanation surface is evident at ~1.6 km. One of several isolated peaks that rise to ~2 km is shown on this section.

the slip (Fig. 2a), with greater slip (up to 25 m) allowed if the fault is buried more deeply. Slip of less than 10 m, however, produces significantly worse fits to the observations. The dip of the fault and the rake of the slip are constrained to within 15° by the distribution of shear strains (Fig. 2a); specifically, a dip of less than 45° would produce strains in the northern network that are excluded by the data. The NNE–SSW compressional strain implied by our rupture is consistent with the P axes of smaller earthquakes in the region during this century[15,16,17].

The maximum depth of the lower edge of the rupture is not well constrained by the observations (Fig. 2a). The geodetic data suggest that rupture extended to a depth of at least 35 km, and may well have cut through to the base of the crust (Fig. 3), here estimated to lie at 43–46 km depth[18]. This suggestion is consistent with the evidence that earthquakes occur to depths of 30–50 km beneath the Shillong plateau[15]. The unusually high ratio of slip to fault length implies a static stress drop at the high end of the observed range, consistent with the violence of the event. It was in this earthquake that, for the first time, accelerations exceeding 1*g* were identified as responsible for propelling objects into the air. From European seismograms, Richter calculated a surface-wave magnitude of $M_s = 8.7$ although retrospective calibration of these same records yields $M_s = 8.0 \pm 0.1$ (ref. 19). The parameters of the rupture shown in Fig. 2 correspond to moment magnitude $M_w = 8.1$.

The triangulation data exclude significant slip on the Dauki fault, at the southern margin of the plateau, during the 1897 event. The question remains as to whether this undoubtedly major fault[20,21] is a Himalayan thrust fault, as previous interpretations of the 1897 event have concluded. In Miocene times this fault accommodated westward translation of the Indo–Burman ranges[22], but, increasingly since Pliocene times, the fault has permitted reverse slip. If the Dauki fault is, indeed, a major fault bounding the plateau, then it is reasonable to assume that, like the Oldham fault, it cuts to the base of the crust. If the Dauki fault were a gently dipping thrust fault (6°–15° N) it would intersect the Oldham fault in the mid-crust (6–14 km) (Fig. 3). For the two faults not to intersect within the crust, the Dauki fault would need to dip at more than 40°.

We therefore interpret the Shillong plateau as a pop-up structure bounded by (at least) two reverse faults (Fig. 3). This interpretation is consistent with, but not required by, gravity data that suggest the plateau is uncompensated[15,18]. It is unclear why the Shillong plateau should be the only major pop-up structure in the northern Indian shield. The in-plane compressional stress is principally responsible for driving the uplift of the plateau, yet the associated flexure due to the bending of the Indian plate may contribute to the initiation and/or sustenance of plateau pop-up. Moreover, two major loads on the lithosphere are present here that are absent elsewhere along the Himalayan chain: the sediments of the Bengal fan are up to 23 km thick to the south and east of the plateau (Fig. 3), and the Indo–Burman ranges represent an overthrust load that is moving westwards over the Indian lithosphere[22]. Either, or both, of these loads may amplify the stresses already acting on the Indian plate due to the load of the Himalaya. Alternatively, the explanation may lie in a pre-existing heterogeneity; the Miocene strike-slip Dauki fault may have nucleated dip-slip faulting as the region approached the Himalaya in Pliocene times.

We now estimate the rate of uplift and shortening of the Shillong plateau. The time of uplift of this plateau has been inferred from a coarsening of sediment lithology that starts in the Pliocene (2–5 Myr ago)[21]. The surface of the 2-km-high plateau consists of Archaean rocks, and equivalent rocks lie 4–5 km below sea level to the north and south of the plateau[22] (Fig. 3). The mean surface level of the Shillong plateau is approximately horizontal (Fig. 2c), indicating that the cumulative vertical contributions of slip on the Dauki and Oldham faults have been similar since the plateau began to emerge. If we assume that the relative vertical displacement between the top of the Archaean rocks on the plateau, and their equivalents to north and south, has been caused by slip on those faults over the past 2–5 Myr, then a rate of vertical displacement of $2.5 \pm 1\ \mathrm{mm\ yr^{-1}}$ is implied on each of the faults. Assuming they each dip at 50°, these rates translate into fault slip rates of $3.3 \pm 1.3\ \mathrm{mm\ yr^{-1}}$ and to horizontal shortening rates of $4 \pm 2\ \mathrm{mm\ yr^{-1}}$ on the two faults combined. These estimates are consistent with 1997–99 GPS measurements that indicate the central Shillong plateau moves south at a rate of $6.3 \pm 3.8\ \mathrm{mm\ yr^{-1}}$ relative to points in central and southern India[23].

From these rates we estimate a recurrence interval for earthquakes resembling the 1897 event (slip of 15 m) to be 3–8 kyr on each fault. Palaeoseismic investigations along the northern edge of the plateau indicate a 500-year interval between the past four high-intensity shaking events[24], but these may record accelerations from moderate local earthquakes and large events in the Bhutan Himalaya, in addition to events of 1897 type.

Our finding of the reverse slip on the Oldham fault ends a century of speculation as to the mechanism of the 1897 earthquake. The Shillong plateau is not being built as part of a system of thin-skinned thrusting, but is bounded by a high-angle reverse fault to its north, and probably also to its south. The Shillong plateau thus resembles the pop-up structures that border thrust belts elsewhere[25]. The Shillong faults, and the smaller high-angle compressional faulting in the foreland of the entire Himalayan arc, are located in the region flexed by the load of the Himalaya[26]. This association implies that the mechanical cause of the deformation is a superposition of elastic stresses caused by bending of the Indian plate and in-plane compressional stress from India's collision with Tibet. As pointed out by Rogers[25], most if not all of such structures are, or were when active, near to large mountain chains that could have provided the same state of stress that drives the uplift of the Shillong plateau.

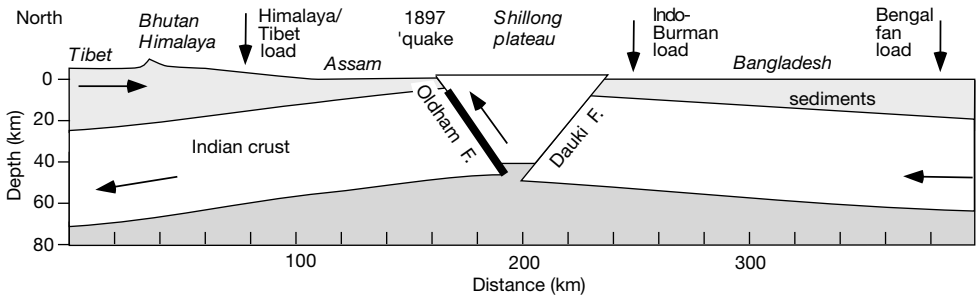

Figure 3 North–south section from Tibet to the Bay of Bengal showing schematic geometry of plateau pop-up. Although the dip of the Dauki fault is conjectural, it would intersect the 1987 rupture were its dip less than ~40°, resulting in a geometry that is incompatible with continued slip on both faults. Slip is inhibited[32] on reverse faults with dip greater than 50°.

There is thus no need to invoke basal tractions due to subduction to explain pop-up structures, as has often been done for the western Americas[27,28,29].

The absence of slip beneath the Bhutan Himalaya in 1897 suggests that the 400-km region between the great Himalayan ruptures of 1934 and 1950 (Fig. 1) has remained a seismic gap for at least the past two centuries[30]. At the higher end of our estimated slip rates, the faults bounding the Shillong plateau could absorb one-third of the inferred Himalayan contraction rate of 18 mm yr^{-1} (ref. 31), correspondingly increasing the interval between great earthquakes in the Bhutan Himalaya.

Our conclusions also raise issues concerning the seismic hazard potential of the Shillong plateau. The >300-km length of the Dauki fault has not slipped recently, but were it to slip in a single earthquake its potential maximum magnitude ($M \geq 8$) would constitute a significant seismic threat to nearby densely populated regions of Bangladesh, and to the very large city of Dhaka less than 150 km to the south (Fig. 1). The interval between these giant plateau-building earthquakes fortunately exceeds 3,000 years. □

Received 1 September 2000; accepted 31 January 2001.

1. Oldham, R. D. Report on the Great Earthquake of 12 June 1897. *Mem. Geol. Soc. India* **29,** 1–379 (1899).
2. Seeber, L. & Armbruster, J. in *Earthquake Prediction: An International Review* (eds Simpson, D. W. & Richards, P. G. 259–277 (Maurice Ewing Series, Vol. 4, American Geophysical Union, Washington DC, 1981).
3. Molnar, P. & Pandey, M. R. Rupture zones of great earthquakes in the Himalayan Region. *Proc. Indian Acad. Sci. (Earth Planet. Sci.)* **98,** 61–70 (1989).
4. Molnar, P. The distribution of intensity associated with the great 1897 Assam earthquake and bounds on the extent of the rupture zone. *J. Geol. Soc. India* **30,** 13–27 (1987).
5. Gahalaut, V. K. & Chander, R. A rupture model for the great earthquake of 1897, northeast India. *Tectonophysics* **204,** 163–174 (1992).
6. Bond, J. in *Annual Report of Triangulation 1897–1898* (ed. Strahan, C.) Part II, xii–xiii (Survey of India Department, Calcutta, 1899).
7. Burrard, S. G. *Great Trigonometrical Survey of India, North East Longitudinal Series, Synoptical Volume 35* (Survey of India, Dehra Dun, 1909).
8. Wilson, C. A. K. *Triangulation of the Assam Valley Series, Geodetic Report 1938*, 10–22 (Survey of India, Dehra Dun, 1939).
9. Strahan, G. *Great Trigonometrical Survey of India, Assam Valley Triangulation, Synoptical Volume 32* (Survey of India, Calcutta, 1891).
10. Nagar, V. K., Singh, A. N. & Prakesh, A. Strain pattern in N. E. India inferred from geodetic triangulation data. *Mem. Geol. Soc. India* **23,** 265–273 (1992).
11. Frank, F. C. Deduction of earth strains from survey data. *Bull. Seismol. Soc. Am.* **56,** 35–42 (1966).
12. Okada, Y. Surface deformation due to shear and tensile faults in a half-space. *Bull. Seismol. Soc. Am.* **75,** 1135–1154 (1985).
13. Das, J. D., Saraf, A. K. & Jain, A. K. Fault tectonics of the Shillong Plateau and adjoining regions, northeast India, using remote sensing. *Int. J. Remote Sensing* **16,** 1633–1646 (1995).
14. Gomberg, J. & Ellis, M. Topography and tectonics of the central New Madrid seismic zone: results of numerical experiments using a three-dimensional boundary element program. *J. Geophys. Res.* **99,** 20299–20310 (1994).
15. Chen, W.-P. & Molnar, P. Source parameters of earthquakes and intraplate deformation beneath the Shillong Plateau and the northern Indoburman ranges. *J. Geophys. Res.* **95,** 12527–12552 (1990).
16. Le Dain, A. Y., Tapponier, P. & Molnar, P. Active faulting and tectonics of Burma and surrounding regions. *J. Geophys. Res.* **89,** 453–472 (1984).
17. Khattri, K. N. Seismological investigations in north eastern region of India. *Mem. Geol. Surv. India* **23,** 275–302 (1992).
18. Verma, R. K. & Mukhopadhay, M. An analysis of the gravity field in northeastern India. *Tectonophysics* **42,** 283–317 (1977).
19. Ambraseys, N. Reappraisal of North Indian earthquakes at the turn of the 20th century. *Current Sci.* **79,** 1237–1250 (2000).
20. Murthy, M. V. N., Talukdar, S. C., Bhattacharya, A. C. & Chakrabarti, C. The Dauki Fault of Assam. *Bull. Oil Natural Gas Commission* **6,** 57–64 (1969).
21. Johnson, S. J. & Alam, A. M. N. Sedimentation and tectonics of the Sylhet trough, Bangladesh. *Geol. Soc. Am. Bull.* **103,** 1513–1527 (1991).
22. Evans, P. The tectonic framework of Assam. *J. Geol. Soc. India* **5,** 80–96 (1964).
23. Paul, J. *et al.* Active deformation across India. *Geophys. Res. Lett.* **28,** 647–651 (2001).
24. Sukhija, B. S. *et al.* Timing and return of major paleoseismic events in the Shillong Plateau, India. *Tectonophysics* **308,** 53–65 (1999).
25. Rogers, J. Chains of basement uplifts within cratons marginal to orgenic belts. *Am. J. Sci.* **287,** 661–692 (1987).
26. Lyon-Caen, H. & Molnar, P. Gravity anomalies, flexure of the Indian Plate, and the structure, support and evolution of the Himalaya and Ganga basin. *Tectonics* **4,** 513–538 (1985).
27. Lipman, P. W., Protska, H. J. & Christiansen, R. L. Evolving subduction zones in the western United States, as interpreted from igneous rocks. *Science* **174,** 821–825 (1971).
28. Dickinson, W. R. & Snyder, W. S. Plate tectonics of the Laramide orogeny. *Geol. Soc. Am. Mem.* **151,** 355–366 (1978).
29. Jordan, T. E. *et al.* Andean tectonics related to the geometry of the subducted Nazca plate. *Geol. Soc. Am. Bull.* **94,** 341–361 (1983).
30. Bilham, R. & Gaur, V. K. The geodetic contribution to Indian seismotectonics. *Current Sci.* **79,** 1259–1269 (2000).
31. Bilham, R., Larson, K., Freymueller, J., & Project Idylhim members. GPS measurements of present-day convergence across the Nepal Himalaya. *Nature* **386,** 61–64 (1997).
32. Sibson, R. H. & Xie, G. Dip range for intracontinental reverse fault ruptures: the truth not stranger than friction. *Bull. Seismol. Soc. Am.* **88,** 1014–1022 (1998).

Acknowledgements

This work was funded by the National Science Foundation and the Natural Environment Research Council. R.B. received a John Simon Guggenheim Memorial Foundation fellowship while at Oxford University.

Correspondence and requests for materials should be addressed to R.B. (e-mail: bilham@stripe.colorado.edu).

Plant diversity enhances ecosystem responses to elevated CO_2 and nitrogen deposition

Peter B. Reich*, Jean Knops†, David Tilman†, Joseph Craine‡, David Ellsworth§, Mark Tjoelker*, Tali Lee*, David Wedin‖, Shahid Naeem†, Dan Bahauddin*, George Hendrey§, Shibu Jose*, Keith Wrage*, Jenny Goth* & Wendy Bengston*

* *Department of Forest Resources, University of Minnesota, St Paul, Minnesota 55108, USA*
† *Department of Ecology, Evolution and Behavior, University of Minnesota, St Paul, Minnesota 55108, USA*
‡ *Department of Integrative Biology, University of California, Berkeley, California 94720, USA*
§ *Division of Environmental Biology, Brookhaven National Laboratory, Upton, New York 11973, USA*
‖ *School of Natural Resource Sciences, University of Nebraska, Lincoln, Nebraska 68583, USA*

Human actions are causing declines in plant biodiversity, increases in atmospheric CO_2 concentrations and increases in nitrogen deposition; however, the interactive effects of these factors on ecosystem processes are unknown[1,2]. Reduced biodiversity has raised numerous concerns, including the possibility that ecosystem functioning may be affected negatively[1–4], which might be particularly important in the face of other global changes[5,6]. Here we present results of a grassland field experiment in Minnesota, USA, that tests the hypothesis that plant diversity and composition influence the enhancement of biomass and carbon acquisition in ecosystems subjected to elevated atmospheric CO_2 concentrations and nitrogen deposition. The study experimentally controlled plant diversity (1, 4, 9 or 16 species), soil nitrogen (unamended versus deposition of 4 g of nitrogen per m^2 per yr) and atmospheric CO_2 concentrations using free-air CO_2 enrichment (ambient, 368 μmol mol^{-1}, versus elevated, 560 μmol mol^{-1}). We found that the enhanced biomass accumulation in response to elevated levels of CO_2 or nitrogen, or their combination, is less in species-poor than in species-rich assemblages.

In the twenty-first century humans will live in, manage and depend on ecosystems that are less diverse[1,2] and subjected to higher CO_2 levels and nitrogen (N) deposition rates than in recorded human history[1]. Although we are beginning to understand the individual impacts of each of these factors on terrestrial ecosystems, our understanding of their interactive effects is poor at best[1–10]. Net primary productivity and carbon (C) input to ecosystems are usually enhanced by elevated CO_2, but this seems to be related to the extent and type of other limitations[11–20]. Nitrogen-poor ecosystems have often shown less response to elevated CO_2 than more fertile systems[18–25], which is important given that, worldwide,